

See discussions, stats, and author profiles for this publication at: <https://www.researchgate.net/publication/355370021>

UV and IR Laser-Patterning for High-Density Thin-Film Neural Interfaces

Conference Paper · September 2021

DOI: 10.23919/EMPC53418.2021.9584962

CITATIONS

0

READS

52

9 authors, including:



Andrada Velea

Delft University of Technology

5 PUBLICATIONS 8 CITATIONS

[SEE PROFILE](#)



Joshua Wilson

The University of Manchester

24 PUBLICATIONS 316 CITATIONS

[SEE PROFILE](#)



Anna Pak

Delft University of Technology

3 PUBLICATIONS 13 CITATIONS

[SEE PROFILE](#)



Nasim Bakhshae

Delft University of Technology

3 PUBLICATIONS 1 CITATION

[SEE PROFILE](#)

Some of the authors of this publication are also working on these related projects:



Informed Project <http://informed-project.eu> [View project](#)



Education in Electrical Engineering and Biomedical Engineering [View project](#)

UV and IR Laser-Patterning for High-Density Thin-Film Neural Interfaces

Andrada I. Velea^{1,2}, *Student Member, IEEE*, Joshua Wilson², Anna Pak^{1,2}, Manuel Seckel³, Sven Schmidt³, Stefan Kosmider³, Nasim Bakhshaei¹, Wouter A. Serdijn¹, *Fellow, IEEE*, and Vasiliki Giagka^{1,2}, *Member, IEEE*

¹Bioelectronics Section, Department of Microelectronics, Delft University of Technology, Delft, The Netherlands,

²Technologies for Bioelectronics Group, Department of System Integration and Interconnection Technologies, Fraunhofer IZM, Berlin, Germany,

³Embedding and Substrate Technologies Group, Department of System Integration and Interconnection Technologies, Fraunhofer IZM, Berlin, Germany

Corresponding authors e-mails: a.velea-1@tudelft.nl, v.giagka@tudelft.nl

Abstract— Our limited understanding of the nervous system forms a bottleneck which impedes the effective treatment of neurological disorders. In order to improve patient outcomes it is highly desirable to interact with the nervous tissue at the resolution of individual cells. As neurons number in the billions and transmit signals electrically, high-density, cellular-resolution microelectrode arrays will be a useful tool for both treatment and research.

This paper investigates the advantages and versatility of laser-patterning technologies for the development of such high-density microelectrode arrays in flexible polymer substrates. In particular, it aims to elucidate the mechanisms involved in laser patterning of thin polymers on top of thin metal layers. For this comparative study, a pulsed picosecond laser (Schmoll Picodrive) with two separate wavelengths (1064 nm (infrared (IR)) and 355 nm (ultraviolet (UV))) was used. A 5 μm thick electroplated layer of gold (Au) was used to form the microelectrodes. Laser-patterning was investigated to expose the Au electrodes when encapsulated by two different thermoplastic polymers: thermoplastic polyurethane (TPU), and Parylene-C, with thicknesses of maximum 25 μm . The electrode diameter and the distance between electrodes were reduced down to 35 μm and 30 μm , respectively. The structures were evaluated using optical microscopy and white light interferometry and the results indicated that both laser wavelengths can be successfully used to create high-density microelectrode arrays in polymer substrates. However, due to the lower absorption coefficient of metals in the IR spectrum, a higher uniformity of the exposed Au layer was observed when IR-based lasers were used. This paper provides more insight into the mechanisms involved in laser-patterning of thin film polymers and demonstrates that it can be a reliable and cost-effective method for the rapid prototyping of thin-film neural interfaces.

Keywords—high-density microelectrode arrays, thin-film laser drilling, polyurethane, Parylene-C.

I. INTRODUCTION

In the past few decades, neuromodulation has been widely investigated as a means to develop tailored approaches for treating various neurological disorders. However, the degree of personalisation that can currently be achieved is hampered by the limited understanding of the mechanisms that govern our

nervous system. To overcome this, it is of paramount importance to increase the resolution at which we interact with the nervous tissue.

To this end, high-density microelectrode arrays are needed. In particular, flexible, polymer-based arrays that seamlessly interface with the neural tissue have the potential for chronic use [1]. To achieve high resolution patterns, photolithography is the method of choice. However, when the electrodes have to be exposed, if photolithography is employed, the designs of the photomasks must be fixed and changes require the fabrication of new masks, making it an expensive approach for prototyping. Alternatively, the use of laser systems, which are single step processes and can create arbitrary patterns for rapid prototyping, can be used [2].

The aim of this study is to go beyond the state of the art and make use of the versatility provided by laser-patterning technologies to develop miniaturised, polymer-based high-density electrode arrays, using thin noble metals as conductors within thin and flexible encapsulation layers. To this end, this paper focuses on investigating the use of laser-patterning alone for biocompatible polymers that can be used in such neural interfaces.

More than a decade ago, it was shown that 18 μm thick platinum (Pt) electrodes with diameters of 50 μm and encapsulated in 20 μm thick silicone rubber could be patterned using a nanosecond laser system, with a 532 nm wavelength [3]. More recently, structures comprising 6, 25 μm thick platinum/iridium (PtIr) electrodes with a diameter of 80 μm , 300 μm pitch between them and encapsulated in 10 μm of Parylene-C were successfully patterned, using a picosecond laser, with a 355 nm wavelength [4]. However, for flexible and conformal high-density arrays, smaller diameters and thinner metal layers are of interest.

Recently, an attempt to develop such thin neural interfaces combined femtosecond laser-patterning (with a 342 nm wavelength) with conventional lithography (plasma etching of polymers). In [5], electrodes of 40 μm in diameter and 500 μm

*This work is part of the Moore4Medical project funded by the ECSEL Joint Undertaking under grant number H2020-ECSEL-2019-IA-876190.

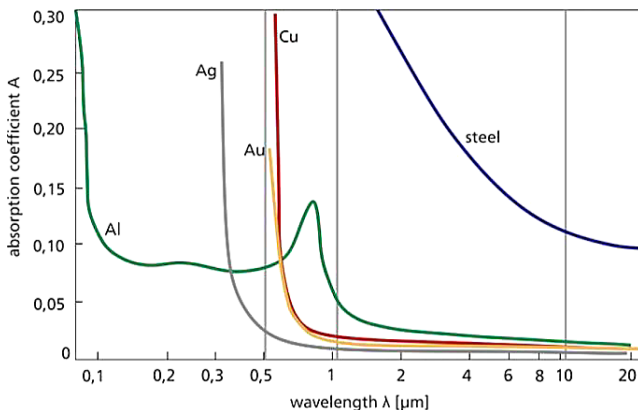


Fig. 1. Absorption coefficient of different metals. Image adjusted from [7].

pitch, using nm thick metal layers and a polyimide insulation layer of 10 μm or 15 μm , were developed.

In this paper, for the development of thin-film, polymer-based microelectrode arrays, as well as for investigating the limitations imposed by such technologies, a pulsed picosecond laser (Schmoll Picodrill) with two separate wavelengths (1064 nm and 355 nm) was used. The minimum beam diameter is $\sim 15 \mu\text{m}$ for the ultraviolet (UV) beam path and $\sim 40 \mu\text{m}$ for the infrared (IR) one. For the test structures, resembling high-density electrode arrays, a 5 μm thick electroplated layer of gold (Au), encapsulated in thin film polymers, was used. For the encapsulation, two different thermoplastic polymers were investigated: thermoplastic polyurethane (TPU) and Parylene-C, with a thickness of maximum 25 μm . The targeted electrode diameter as well as the distance between electrodes were reduced down to 35 μm and 30 μm , respectively. For comparative reasons, thicker polymers (100 μm) as well as larger diameters (700 μm) were also included in the study.

Since this technology aims to ease the fabrication process of dense microelectrode arrays, it is of paramount importance to ensure high quality for both the metal and encapsulation layers. The different wavelengths were selected in order to compare the performance of fundamentally different ablation mechanisms. IR beams generally cause thermal-induced degradation of polymers whereas UV beams have sufficient energy to induce a chemical reaction, causing the polymeric bonds to break [6]. In the IR spectrum, due to the melting of thermoplastic materials,

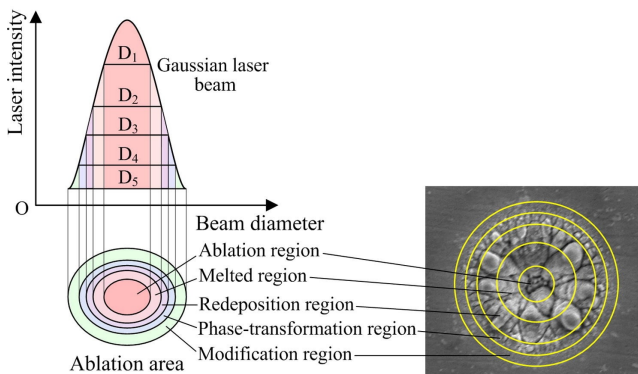


Fig. 2. Diameter variation for a picosecond laser depending on the intensity of the beam. Figure adapted from [8].

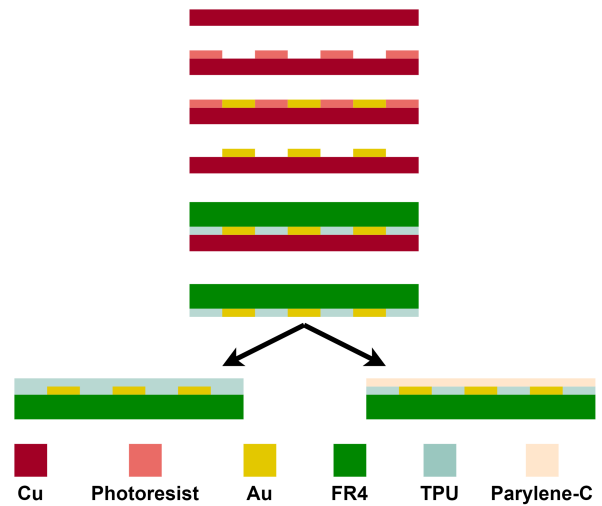


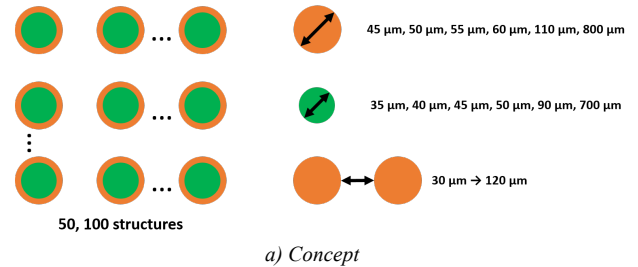
Fig. 3. Fabrication flow used for the development of the test structures.

a reflow phenomenon followed by a partial redeposition of the material can occur. Although the UV beams might be more beneficial for polymers, the absorption coefficient for metals is much larger in the UV spectrum, whereas in IR, the absorption coefficient for Au is almost zero (Fig. 1) [7].

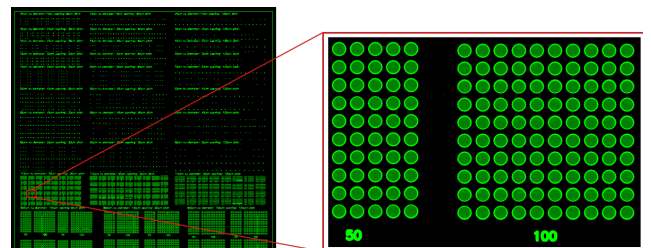
II. METHODS

A. Laser technology

The laser used for these investigations, comparable with what has previously been reported, is a pulsed picosecond laser (Schmoll Picodrill) with a frequency range from 200 kHz up to 1 MHz.



a) Concept



b) Actual design

Fig. 4. Test structures used for laser-patterning (a-concept and b-actual design). The diameters of the metal as well as the diameters of the opening in the polymer layer were varied between 45 – 800 μm and 35 – 700 μm respectively. The distance between electrodes was also varied from 30 – 120 μm .

TABLE 1: Parameters used during the laser-patterning method.

Diameter	Power					
	TPU (UV laser)			Parylene-C (UV laser)		
			Average (W)			Average (W)
hatched mode 35 μm diameter	0.5W every 4th pulse	3 loops	0.375	0.5W every 4th pulse	4 loops	0.5
hatched mode 40 μm diameter	0.5W every 4th pulse	3 loops	0.375	0.7W every 2nd pulse	1 loop	0.35
hatched mode 45 μm diameter	1W every 4th pulse	2 loops	0.5	1W/0.4W every 2nd pulse	1 loop each	0.7
hatched mode 50 μm diameter	1W every 4th pulse	2 loops	0.5	1W/0.4W every 2nd pulse	1 loop each	0.7
hatched mode 90 μm diameter	1W every 4th pulse	2 loops	0.5	1W/0.4W every 2nd pulse	1 loop each	0.7
punched mode	0.5 W every 4th pulse	10 loops	1.25	0.5 W every 4th pulse	9 loops	1.12
	TPU (IR laser)			Parylene-C (IR laser)		
			Average (W)			Average (W)
hatched mode 35 μm diameter	1.5W every 4th pulse	2 loops	0.75	1.5W every 2nd/ 1W every 4th pulse	1 loop each	1
hatched mode 40 μm diameter	1.5W every 4th pulse	2 loops	0.75	1.5W every 2nd/ 1.3W every 4th pulse	1 loop each	1
hatched mode 45 μm diameter	1.5W every 4th pulse	2 loops	0.75	1.5W every 2nd/ 1.3W every 4th pulse	1 loop each	1
hatched mode 50 μm diameter	1.5W every 4th pulse	2 loops	0.75	1.5W every 2nd/ 1.5W every 4th pulse	1 loop each	1.1
hatched mode 90 μm diameter	1.5W every 4th pulse	2 loops	0.75	1.5W every 2nd/ 1.5W every 2nd/ 1.5W every 4th pulse	1 loop each	1.8
punched mode	3W every 4th pulse	4 loops	3	2.5 W every second pulse	2 loops	2.5

The laser uses two separate beam paths. The IR beam has a maximum power of 50 W and a minimum beam diameter of $\sim 40 \mu\text{m}$, when focused. The second, a UV beam, has a maximum power of 14 W and a minimum beam diameter of $\sim 15 \mu\text{m}$, when focused. Depending on the intensity of the laser beam, different results, such as redeposition of material or melted areas can be observed on the surface of the material under test. Fig. 2 illustrates such an example for a metal surface subjected to laser-patterning [8].

For the Schmolz Picodrill laser, two different drilling modes are available: "punched" and "hatched". With the "punched" mode, the pulsed laser directs its energy to a fixed location and thus, small vias with the diameter of the laser beam can be created. The "hatched" option, on the other hand, is used when larger openings, with diameters $> 30 \mu\text{m}$ are desired. In this case, the pulsed laser moves and directs its energy over a predefined area.

B. Materials

For the microelectrode arrays to induce as little damage as possible to the tissue, it is of great importance to have thin, flexible and conformal materials. Therefore, this paper presents the use of polymers for encapsulation purposes and thin Au

layers for the development of the electrodes. Recent publications, employing similar laser-patterning technologies use metal layers with a minimum thickness of $18 \mu\text{m}$ and encapsulation layers down to $10 \mu\text{m}$ [3].

In this work, the targeted metal is a $5 \mu\text{m}$ thick electroplated Au layer while for the encapsulation, two different thermoplastic materials are used: a thermoplastic polyurethane type (Platilon 4201AU, from Covestro), with a thickness of $25 \mu\text{m}$ and a Parylene-C, deposited using Parylene-C dimers from Special Coating Systems with a maximum thickness of $20 \mu\text{m}$.

C. Fabrication of test structures

The fabrication of samples comprised of several steps as illustrated in Fig. 3.

Since the conductive Au layer is deposited by means of electroplating, a thin ($70 \mu\text{m}$) copper (Cu) substrate is needed to ensure the transfer of metal ions, during the process. The Cu substrate was roughened by chemical etching and dried in an oven at $55 \text{ }^\circ\text{C}$ for 30 minutes. Next, a layer of dry negative photoresist (RD-1225) was applied on top of Cu, patterned, using laser direct imaging (LDI), and developed.

Later, Au was electroplated on the defined areas and the photoresist mask was finally removed. Before encapsulation, the structures had to be transferred on a rigid carrier. To this end, epoxy-glass sheets (FR4) were used and laminated, using an intermediate TPU layer, on top of the electroplated structures. As Cu does not fulfil the biocompatibility requirements for implantable devices, the backside Cu layer was etched in copper chloride (CuCl_2), hydrogen chloride (HCl) and hydrogen peroxide (H_2O_2) at $49 \text{ }^\circ\text{C}$ and later rinsed in deionized water.

For the encapsulation, two different processes were used. One consisted of using thermocompression to laminate the TPU material on top of the Au structures, while the other was a chemical vapour deposition process (CVD) for the Parylene-C material.

The TPU lamination was performed at $190 \text{ }^\circ\text{C}$ and 10 bar while the Parylene-C CVD process consisted in the deposition of Parylene monomers onto the surface of interest, at $25 \text{ }^\circ\text{C}$ and 0.05 Torr.

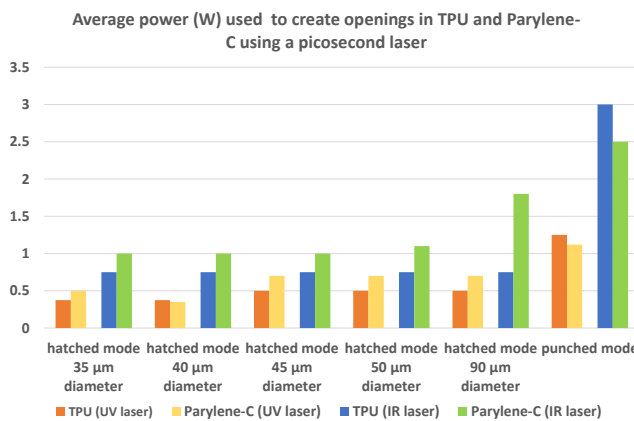


Fig. 5. Average power used for laser-patterning of TPU and Parylene-C.

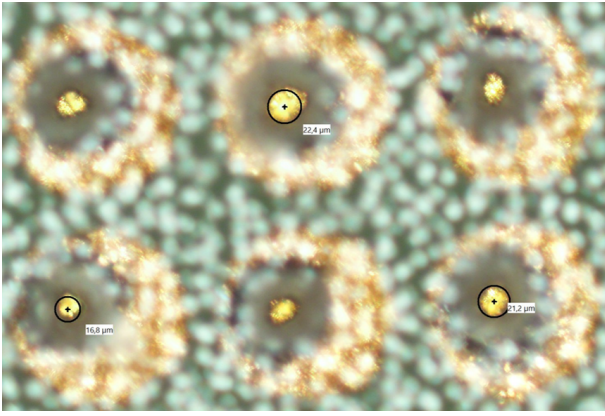


Fig. 6. Openings created in a 20 μm thick Parylene-C layer using an IR laser beam in “punched” mode. The landing material was a 5 μm thick Au layer.

D. Design of test structures

The test structures used in this work (Fig. 4), mimic different design topologies used in the development of flexible microelectrode arrays. The Au electrode diameters were varied from 45 μm to 800 μm in steps of 5 μm , with the exception of the two largest dimensions (110 μm and 800 μm). Similarly, the diameters of the openings in the polymeric layer were varied from 35 μm to 700 μm and the distance between electrodes, was reduced down to 30 μm .

E. Characterisation methods

In order to qualitatively evaluate the patterned structures and the surface of the metal underneath, two characterisation methods were used in combination: *optical microscopy* coupled with *white light interferometry*.

III. RESULTS AND DISCUSSION

The UV and IR lasers were both used to pattern arrays of circles with various diameters and edge-to-edge spacings, in both TPU and Parylene-C. The most important parameters are specified in Table 1. As illustrated, irrespective of the wavelength used, higher average power levels (calculated by (1) and up to 0.2 W higher for the UV laser as well as up to 1.05 W

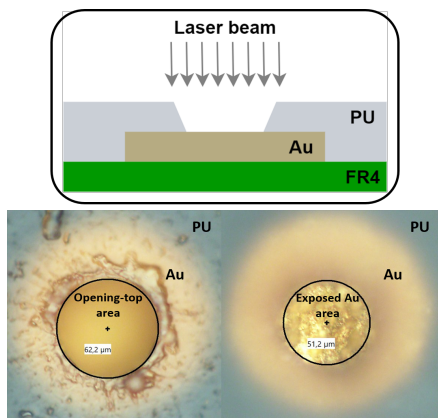


Fig. 7. Representation of the geometrical shape of the opening (top) and its corresponding optical images (bottom).

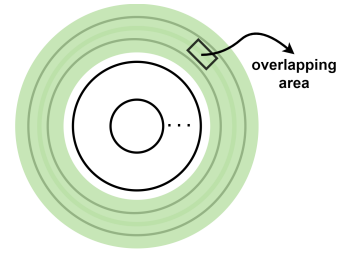


Fig. 8. Rings defining the final opening diameter for the laser-patterning in “hatched” mode.

higher for the IR laser) were needed to create openings in the Parylene-C layer. This is a result of the fundamental differences between the two polymers used. Although both are considered thermoplastic materials and have similar densities, 1.289 g/cm^3 for Parylene-C [9] and 1.15 g/cm^3 for TPU [10], some important differences can be underlined, which are of great importance when using UV or IR lasers.

$$\text{Average Power} = (\text{Power}/ \text{No. Pulses}) * \text{No. Loops} \quad (1)$$

The first one is the melting point of the two materials, an aspect of paramount importance when using IR-based lasers. Parylene-C has a melting point of about 290 $^{\circ}\text{C}$ [9], whereas TPU has a melting point between 155 and 185 $^{\circ}\text{C}$ [10]. Even more important is the chemical composition of the two materials, especially when using UV lasers, for which the ablation mechanism is chemical rather than thermal. Thermoplastic materials are linear polymers with molecular structures comprising molecular bonds organised in a straight-chain formation and thus relatively weak bonds [11]. The third and equally important factor, is the glass transition temperature (T_g) of the two materials, the point at which the reversible transition of the amorphous component from/to a hard and brittle condition to/from a viscous condition occurs. Therefore, the higher the T_g , the less amorphous components the polymers have, meaning that their composition exhibits a more crystalline structure. For TPU, the nominal values of the T_g are between -67 $^{\circ}\text{C}$ and 78.8 $^{\circ}\text{C}$ (according to the ASTM E1356 test method [12]). On the other hand, Parylene-C has a T_g between 80 $^{\circ}\text{C}$ and 100 $^{\circ}\text{C}$ [13], much higher than for TPU, making it more

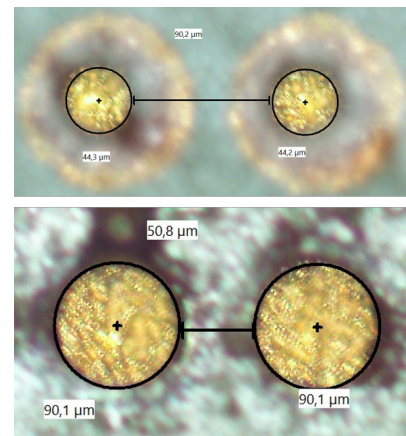


Fig. 9. Openings of different diameters and distances between the electrodes created in a 25 μm thick TPU layer using an IR laser beam in “hatched” mode.

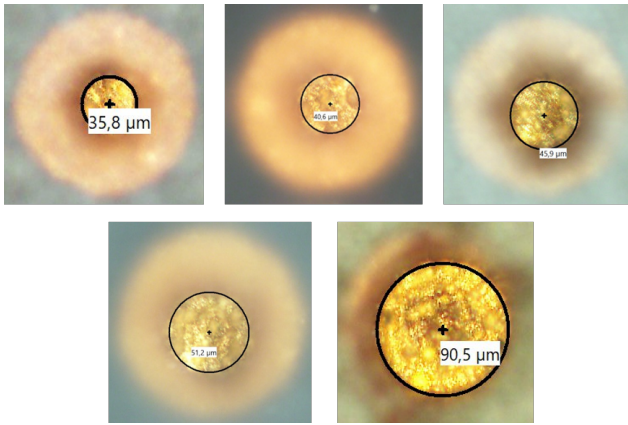


Fig. 10. Openings created in a 25 μm thick TPU layer using a UV laser beam in "hatched" mode. The landing material was a 5 μm thick Au layer.

crystalline. This could, potentially have an influence on the energy needed to break the bonds during a UV-based laser-patterning technology.

Apart from the power values, which differ depending on the material and size of the openings, the frequency at which the laser actively delivers energy to the substrate is another important aspect. However, for small openings, this does not make a difference, although the overall average power (calculated by (1)) is higher.

In Fig. 5, the average power needed for each type of material using either the UV-based or IR-based lasers is shown for different diameters and laser modes.

For the "punched" mode, given the results obtained, clear conclusions cannot be made as the parameters used do not seem to follow the same trend as for the "hatched" mode. Moreover, the diameter of the opening could not be uniformly reproduced, due to the fact that while using the "punched" mode there is no control over the shape of the final opening (Fig. 6).

For the "hatched" mode, the variation observed was mainly dependent on the sizes of the openings and structure of the material. Since the complete opening of each structure as well as the integrity of the metal underneath were the two key factors in determining the suitability of such technology for developing

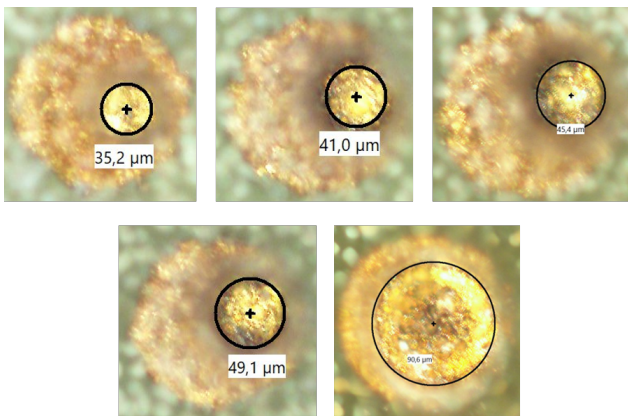


Fig. 11. Openings created in a 20 μm thick Parylene-C layer using a UV laser beam in "hatched" mode. The landing material was a 5 μm thick Au layer.

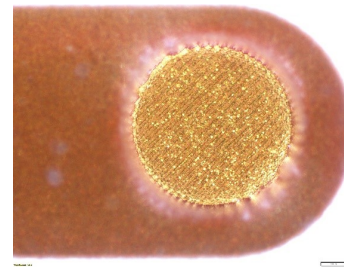


Fig. 12. Opening created in a 100 μm thick TPU layer using a UV laser beam in "hatched" mode. The landing material was a 5 μm thick Au layer.

high-density neural interfaces, the evaluation consisted in acquiring optical images and measuring the depth of the openings using white light interferometry measurements.

Since the intensity of the laser is higher in the center of the beam rather than at the edge, the top area of the opening has a larger diameter compared to the diameter of the exposed Au layer (Fig. 7). To compensate for this and in order to have the desired dimension for the exposed area, the parameters used to define the diameter of the hatched area were slightly larger than the desired ones.

Moreover, when openings larger than the diameter of the laser beam were desired, multiple rings, of different diameters, had to be hatched (Fig. 8). The number of concentric rings needed as well as the distance between them is strongly dependent on the diameter of the beam as an overlap is needed to ensure complete removal of the material. The energy required for the inner rings, especially for Parylene-C, had to be adjusted to ensure a uniform opening.

For both materials and both laser beams, different distances between the openings have been established, ranging from 30 μm to 120 μm and the structures were successfully opened using the same parameters as described in Table 1. An example of such opened structures, having different distances between them is illustrated in Fig. 9.

A. UV laser

UV lasers are known to induce a chemical reaction in the material, which causes polymeric bonds to break, thus leading to a rapid removal of polymer at desired locations. However, depending on the type of polymer and their chemical bonds, the results differ significantly.

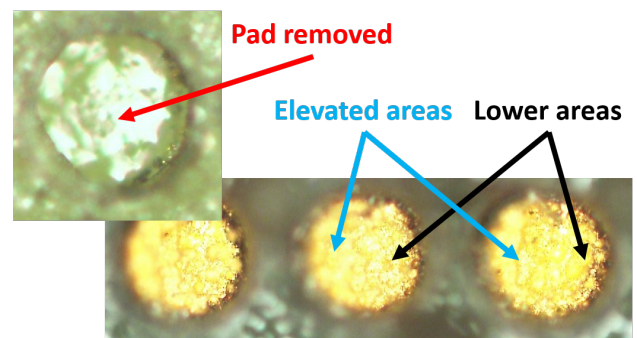


Fig. 13. Damage occurred during the IR-based laser-patterning process due to the different melting points of the layers comprising the structures under test.

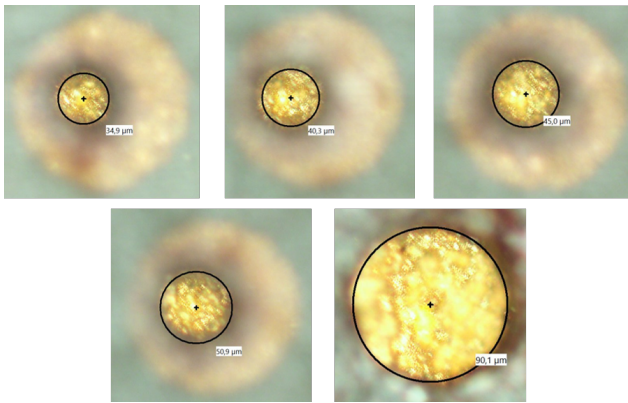


Fig. 14. Openings created in a 25 µm thick TPU layer using an IR laser beam in "hatched" mode. The landing material was a 5 µm thick Au layer.

The investigations conducted using the Schmoll Picodrive laser have shown that for Parylene-C, the removal required double the frequency compared to TPU, to open structures with diameters ranging from 35 µm to 90 µm. This can be seen from the parameters used in both cases, for all diameters, except from the 35 µm one where the difference is not significant and in order to understand the behaviour, in the future, more investigations are needed.

Moreover, since the absorption of metals in the UV spectrum is larger, some polymeric residues could, potentially, still be found on the surface of the electrodes, as more energy or laser-patterning loops would have damaged the Au layer underneath. In order to prove this, inspection methods, such as X-Ray Photoelectron Spectroscopy (XPS) that could evaluate the chemical composition on the surface of the electrodes would be required. However, these investigations were out of scope for the current paper.

From the optical inspection of the patterned structures, dark coloured areas (Fig. 10 and Fig. 11) on the surface of the Au layer were observed after the removal of both materials. These indicated the potential presence of polymeric residues which could also be caused by the roughness of the metal layer. The roughness of Au which can be seen also from the different visible peaks on the exposed areas, is due to the intermediate Cu layer on which Au was electroplated. Nevertheless, to remove such particles, an oxygen plasma cleaning step could be included in the process flow [5].

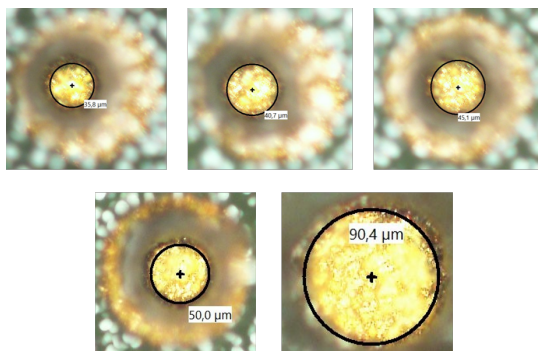


Fig. 15. Openings created in a 20 µm thick Parylene-C layer using an IR laser beam in "hatched" mode. The landing material was a 5 µm thick Au layer.

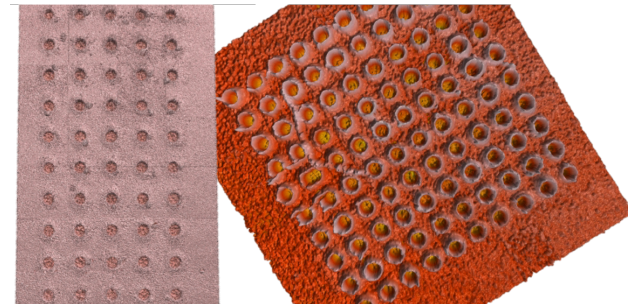
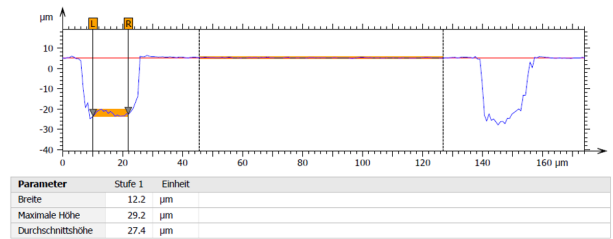


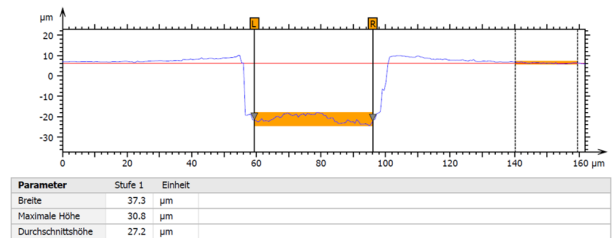
Fig. 16. Arrays comprising of 50 and 100 opened structures.

The misalignment observed for the openings created in Parylene-C (Fig. 11) are caused by the fact that Parylene is slightly opaque after deposition and thus the contrast between Parylene and the Au layer underneath was not always strong enough to be distinguished accurately by the laser camera.

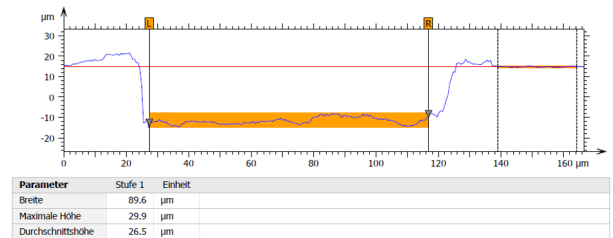
For the sake of comparison, thicker TPU layers (100 µm) with larger diameter openings (700 µm) were investigated. In this case, 10 repetitions with a laser power of 1 W were needed to remove the TPU layer. Since the exposed area is much larger, the Au layer appears to be more uniform in the optical image (Fig. 12). However, the surface roughness caused by the Cu layer on top of which Au was electroplated, is still visible.



a) 25 µm thick TPU openings using the "punched" mode of the laser.

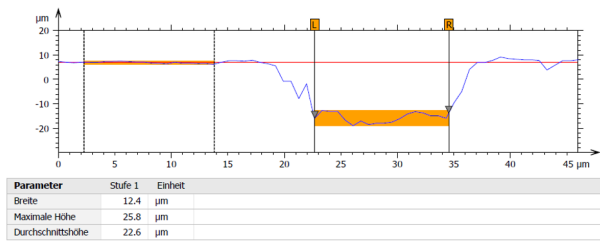


b) A 25 µm thick TPU opening with a diameter of 35 µm.

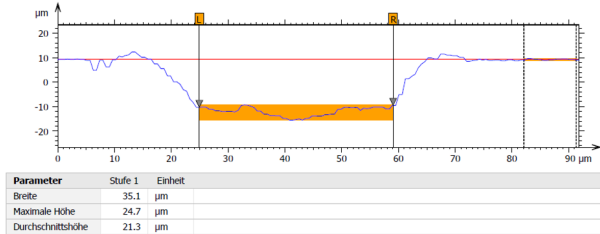


a) A 25 µm thick TPU opening with a diameter of 90 µm.

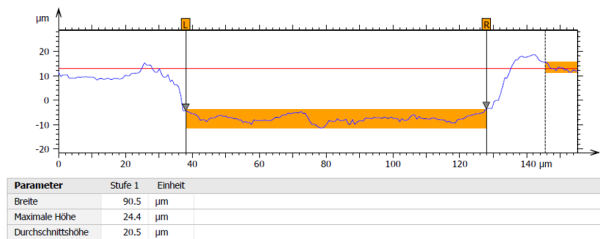
Fig. 17. White light interferometry measurements for TPU openings created using the "punched" or the "hatched" modes of the picosecond laser. The landing material was a 5 µm thick Au layer.



a) 20 μm thick Parylene-C openings using the "punched" mode of the laser.



b) A 20 μm thick Parylene-C opening with a diameter of 35 μm .



b) A 20 μm thick Parylene-C opening with a diameter of 90 μm .

Fig. 18. White light interferometry measurements for Parylene-C openings created using the "punched" or the "hatched" modes of the picosecond laser. The landing material was a 5 μm thick Au layer.

B. IR laser

IR-based laser-patterning induces a thermal ablation of polymers. For Parylene-C, in all cases, higher average power levels were needed and these could, potentially, be even higher for a Parylene-C layer of 25 μm (the same thickness as the TPU layer). Moreover, during this process, failure of some structures was also observed. This was due to the stack of layers the structures consisted of (FR4 - TPU - Au - Parylene-C). Since the melting point for TPU is lower than for Parylene-C, the bottom surface of the structures reached the melting temperature faster than the top surface. Therefore, some of the metal pads were either completely removed or tilted at a certain angle, depending on the reflow of TPU over the entire surface area (Fig. 13).

Nevertheless, diameters ranging from 35 μm to 90 μm were opened using the "hatched" mode of the IR laser, leading to exposed Au areas with an increased uniformity and less residues compared to the UV-based laser (Fig. 14 and Fig. 15). These results are a first indication that IR beams are more suitable for laser-patterning of polymers when the integrity of the thin metal layers underneath is required.

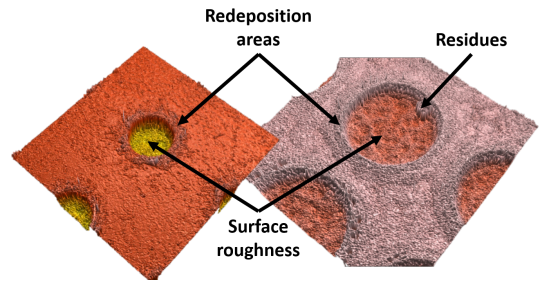


Fig. 19. Circular areas around the hatched or punched regions where polymers have been redeposited. The openings have diameters of 35 μm and 90 μm respectively. The surface roughness of the metal layer is also visible on the reconstructed 3D image.

C. White light interferometry

White light interferometry measurements were used for each of the opened structures to evaluate if the polymeric layer was completely removed for the desired diameter of the exposed Au layer. Fig. 16 illustrates arrays of opened structures comprising of either 50 or 100 elements.

In Fig. 17 and Fig. 18, examples of such measurements are illustrated for openings with diameters of 35 μm and 90 μm in both Parylene-C and TPU using the "hatched" mode of the two different laser beams. Moreover, the openings created using the "punched" mode of the lasers were also measured although their very small diameter varied from one opening to another.

The small peaks observed at the outer ring of the openings are due to the redeposition of polymers at the outside of the lasered area. This has been observed for both types of materials, irrespective of the wavelength used and it becomes more visible on the 3D reconstructed images of the measured samples (Fig. 19).

D. Selected metals and encapsulation materials

This study investigated the use of TPU and Parylene-C as encapsulation materials for Au microelectrodes. Hence, it is far from complete. State-of-the-art neural interfaces make use of other polymers as well (i.e. silicone rubber [14], polyimide [5]) or combinations of ceramics and polymers in encapsulation stacks for packaging purposes ([15], [16], [17]). In addition, Pt or PtIr, or even iridium oxide, PEDOT, and more recently graphene microelectrodes are preferred instead of Au for neural stimulation purposes due to the higher charge storage capacities these materials exhibit. A more complete future study should also include the effect of laser-patterning on these material combinations. A similar behaviour is expected for noble metals, however, for polymer-based electrodes it is expected that such technology is not selective enough and thus, the surface integrity of the electrodes might be compromised. On the other hand, for graphene electrodes, depending on the wavelength used, the technology could, potentially be successful. One of the most commonly used methods to evaluate graphene, without damaging it, is Raman Spectroscopy, which typically uses wavelengths in the range of 500 – 650 nm and as shown in [3], laser-patterning of polymers was possible using a 532 nm wavelength. However, the power levels required to open the

polymer-based encapsulation layers as well as the reduced thickness of graphene, might pose serious limitations for such technologies.

IV. CONCLUSIONS

This paper investigates the advantages and versatility of laser-patterning technologies for the development of high-density microelectrode arrays. In particular, it aims to shine more light into the mechanisms involved in laser patterning of thin polymers on top of thin metal layers. To this end, it presents a comparative patterning study using two distinct laser wavelengths, a UV and an IR beam.

A pulsed picosecond laser was used and diameters ranging from 35 μm to 700 μm were successfully created using both the UV and IR lasers. It has been shown that, by using the IR laser beam, a much higher surface uniformity is achieved due to the low absorption coefficient of Au in the IR spectrum. Moreover, for the UV laser, a redeposition of particles or the presence of residues was more pronounced, in comparison to the IR-based laser-patterned structures. However, this could be overcome by employing oxygen plasma cleaning steps at the end of the process. The white light interferometry results showed that the test structures were completely opened, regardless of the number present on the arrays (50 or 100 structures). Neither did the change in distance among the patterned structures present any changes in the parameters used or the results obtained. To the best of the authors' knowledge, this is the first time that laser-patterning alone was employed for structures comprising such thin metal and encapsulation layers.

Laser-patterning can be a fast, cost-effective and efficient method for the development of high-density, polymer encapsulated microelectrode arrays. The comparative study presented in this work can be useful to increase our understanding and enable an increased adoption of this versatile technology for high-density, thin neural interfaces.

ACKNOWLEDGMENTS

We acknowledge the staff members of Else Kooi Laboratory (EKL) from Delft University of Technology (TU Delft), The Netherlands for helping us with the Parylene-C deposition process and the Embedding and Substrate Technologies Group from Fraunhofer Institute for Reliability and Microintegration IZM, Berlin, Germany for their implication and support offered throughout the project. Special thanks are to be addressed to all our collaborators from the Bioelectronics group at TU Delft.

REFERENCES

- [1] V. Giagka, and W. Serdijn, "Realizing flexible bioelectronic medicines for accessing the peripheral nerves – technology considerations," *Bioelectronic Medicine journal*, vol. 4, no. 8, Jun. 2018. doi: 10.1186/s42234-018-0010-y
- [2] V. Giagka, A. Demosthenous, and N. Donaldson, "Flexible active electrode arrays with ASICs that fit inside the rat's spinal canal," *Biomed. Microdev.*, vol. 17, no. 6, pp. 106 – 118, Dec. 2015. doi: 10.1007/s10544-015-0011-5.
- [3] M. Schuettler, S. Stiess, B. V. King, and G. J. Suaning, "Fabrication of implantable microelectrode arrays by laser cutting of silicone rubber and platinum foil," *Journal of Neural Engineering*, vol. 2, Mar. 2005.
- [4] M. Muller, N. de la Oliva, J. del Valle, I. Delgado-Martinez, X. Navarro, and T. Stieglitz, "Rapid prototyping of flexible intrafascicular electrode arrays by picosecond laser structuring," *Journal of Neural Engineering*, vol. 14, Nov. 2017.
- [5] H-L. Yeh, J. V. Garich, I. R. Akamine, J. M. Blain-Christen, and S. A. Hara, "Laser micromachining of thin-film polyimide microelectrode arrays: alternative process to photolithography," *Proc. 2020 Design of Medical Devices Conference*, Mineapolis, MN USA, Apr. 2020.
- [6] O. Yalukova, and I. Sarady, "Investigation of interaction mechanisms in laser drilling of thermoplastic and thermoset polymers using different wavelengths," *Composites Science and Technology*, vol. 66, pp. 1289-1296, 2006.
- [7] F. Brueckner, M. Riede, M. Müller, F. Marquardt, R. Willner, A. Siedel, E. Lopez, C. Leyens, and E. Beyer, "Enhanced manufacturing possibilities using multi-materials in laser metal deposition," *36th International Congress on Applications of Laser Electro-Optics*, Atlanta, GA USA, Oct. 2017.
- [8] B. Zheng, G. Jiang, W. Wang, X. Mei, and F. Wang, "Surface ablation and threshold determination of AlCu4SiMg aluminum alloy in picosecond pulsed laser micromachining," *Optics and Laser Technology*, vol. 94, pp. 267-278, Sept. 2017.
- [9] Special Coating Systems datasheet: "SCS Parylene Properties – High performance conformal coatings," document link: <https://www.medica.de/vis-content/event-medcom2020.COMPAMED/exh-medcom2020.2670953/COMPAMED-2020-Specialty-Coating-Systems-Inc.-Product-medcom2020.2670953-M3PLFzSgRaGeLx9wk1gizQ.pdf>.
- [10] Covestro Solutions datasheet: "Product Information Plaitlon – High Elastic Polyurethane Films," document link: <https://solutions.covestro.com/en/brands/plaitlon>.
- [11] C. C. Ibeh, "Introduction and History of the Plastics Industry," chapter, *Thermoplastic materials: Properties, Manufacturing Methods, and Applications book*, FL: CRC Press, 2011.
- [12] "Thermoplastics Polyurethane (TPU) Typical Properties Generic TPU, Unspecified," Prospector website, <https://plastics.ulprospector.com/generics/54/c/t/thermoplastic-polyurethane-tpu-properties-processing/sp/2>, last access date: 24.06.2021.
- [13] "Parylene Thermal Properties," Para-Coat Technologies (PCT) website, <https://pctconformalcoating.com/parylene/parylene-thermal-properties/>, last access date: 24.06.2021.
- [14] M. Schuettler, S. Stiess, B. V. King, and G. J. Suaning, "Fabrication of implantable microelectrode arrays by laser cutting of silicone rubber and platinum foil," *Journal of Neural Engineering*, vol. 2, Mar. 2005.
- [15] C. Lamont, T. Grego, K. Nanbakhsh, A. Shah Idil, V. Giagka, A. Vanhoestenbergh, S. Cogan, and N. Donaldson, "Silicone encapsulation of thin-film SiO_x, SiO_xN_y and SiC for modern electronic medical implants: a comparative long-term ageing study", vol. 18, no. 5, pp 055003, 2021. doi: 10.1088/1741-2552/abfd06
- [16] K. Nanbakhsh, R. Ritasalo, W. A. Serdijn and V. Giagka, "Long-term encapsulation of platinum metallization using a HfO₂ ALD - PDMS bilayer for non-hermetic active implants," in *Proc. IEEE Electron. Comp. Tech. Conf. (ECTC) 2020*, Orlando, FL, USA, May 2020. doi: 10.1109/ECTC32862.2020.00081
- [17] X. Xie, L. Rieth, R. Caldwell, M. Diwekar, P. Tathireddy, R. Sharma and F. Solzbacher, "Long-term bilayer encapsulation performance of atomic layer deposited Al₂O₃ and Parylene C for biomedical implantable devices," *IEEE Trans. Biomed. Eng.* vol. 60, no. 10, pp. 2943-51, Jun. 2013.